Catalysis Letters 19 (1993) 351–360

Effect of grain size on the synthesis of active alumina from gibbsite by flash calcination and rehydration

Peter T. Tanev [1] and Lyubomir T. Vlaev

Department of Chemical Engineering, Bourgas University of Technology,
Bourgas 8010, Bulgaria

Received 14 September 1992; accepted 15 April 1993

Two series of alumina have been prepared by flash calcination (FCAL) and subsequent rehydration of "coarse" (> 50 μm) and "fine" grain size gibbsite (< 50 μm). The initial grain size of the gibbsite was found to determine the degree of amorphization, water content, rehydration ability, composition and pore structure of FCAL products. Active alumina materials having pore structure parameters similar to those of commercial alumina adsorbents and catalyst supports were obtained by FCAL and subsequent rehydration of fine grain size gibbsite.

Keywords: Gibbsite; flash calcination; rehydration; pore structure; grain size effect; active alumina preparation

1. Introduction

Gibbsite, prepared as an intermediate by the Bayer process [1], provides a low cost route to activated aluminum oxide (AAO) for use as an adsorbent and catalyst support in petrochemistry. At present only a few methods for AAO preparation from gibbsite are known. These include dissolution followed by precipitation [2,3]; mechanical activation [4,5]; long-time vacuum calcination [6,7]; and short-time (flash) calcination at atmospheric pressure (FCAL) followed by rehydration [8–10]. The disadvantages of the first three methods are the large amount of energy and the expensive equipment required, the long activation time, and the discontinuous nature of the process. At present the FCAL/rehydration method is considered as a promising, low-cost and efficient method for AAO preparation. The initial grain size of gibbsite may affect the efficiency of the FCAL process, i.e. the morphology, rehydration ability, composition, and pore structure of the product. However, the importance of grain size effects is not well investigated. The aim of the

---

[1] To whom correspondence should be addressed. Current address: Department of Chemistry and Center for Fundamental Materials Research, Michigan State University, E. Lansing, MI 48824, USA.

present work is to examine the effect of the initial grain size of gibbsite on AAO preparation by flash calcination and subsequent rehydration.

2. Experimental

A course grain gibbsite from Tuzla, Yugoslavia (designated as CG) having 84% of the particle sizes larger than 50 μm and a synthetic fine grain gibbsite (designated as FG) having 88% of the particles smaller than 50 μm were selected for study. Both samples were subjected to FCAL by pneumatic transport in a vertical tubular oven. The gibbsite mass flow was kept at 1 kg/h by a computer controlled dosing device. Dry air with a velocity of 2700 ℓ/h was used as a transport fluid to ensure particle residence time in the heating zone at 550°C below 1 s.

The FCAL samples were rehydrated at 100°C at a solid : liquid ratio (w/w) of 1 : 10. The rehydration step was carried out at both pH 1.5; and at pH 9.0 [11].

Powder X-ray diffraction patterns were obtained on a TUR M61 diffractometer (Germany) using Ni filtered Cu Kα radiation. Scanning electron micrographs were taken on a PEM-100 Y instrument (USSR). DTG analysis curves were recorded on a MOM Derivatograph (Hungary). The particle size distributions were measured on a Fritsch GmbH sedimentiograph model Analisette 20 using benzene as the dispersing medium.

The specific surface area of the initial gibbsite samples was determined on a instrument designed for low surface area measurements [12]. The full nitrogen adsorption isotherms were measured on a static high vacuum volumetric BET apparatus at −195°C. The specific surface areas (a_{sBET}) and pore volumes (V_p) were determined according to IUPAC recommendations [13]. The prevailing pore sizes ($d_{p,max}$) were obtained from the pore size distribution curves, calculated by the method of Innes [14] using the desorption branch of the isotherms.

3. Results and discussion

The XRD pattern of the FG-FCAL product is quite different from the initial gibbsite (Gb). As shown by the patterns in figs. 1a and 1b the material almost completely transforms to the X-ray amorphous state. In contrast the CG-FCAL sample exhibited little structural changes, as indicated by comparing figs. 1c and 1d. The appearance of the small amount of boehmite (Bö) indicates that the dehydration rate for the course grain material is very low.

The primary particle size of the initial gibbsite, as determined from XRD line width remains unchanged upon FCAL (71.4 and 96.0 nm for FG and CG). However, the secondary particle size decreases (table 1). The scanning electron micrographs presented in fig. 2 support this conclusion. The FG gibbsite (fig. 2a) consists of aggregates of plate-like crystals, which upon FCAL decompose to the smaller

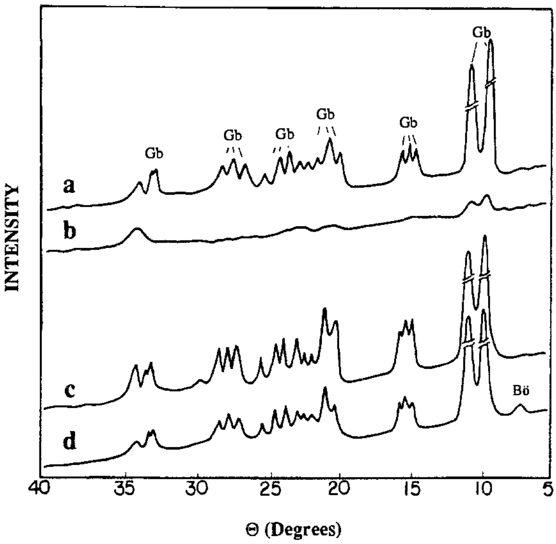

Fig. 1. X-ray diffractograms of samples of (a) initial FG, (b) FG-FCAL, (c) initial CG and (d) CG-FCAL.

particles of sizes 10–30 μm (fig. 2b). In contrast, the CG sample is well crystallized, constituting of monolithic blocks of different sizes and shapes (fig. 2c). An interesting textural change has been observed for the CG-FCAL sample (fig. 2d). In this case FCAL does not lead to visible decomposition of the initial crystal

Table 1

Particle size distributions and pore structure parameters of the initial, FCAL, rehydrated and calcined FG and CG samples

Sample	Particle fraction (wt%)				a_{sBET}	V_p	$d_{p,max}$
	10–20 μm	30–50 μm	50–70 μm	70–90 μm	(m^2/g)	(cm^3/g)	(nm)
FG	21	67	12	–	1.7	–	–
FCAL	60	40	–	–	148	0.09	2.5
rehydrated [a]	12	88	–	–	182	0.19	2.3
calcined [a]	–	–	–	–	258	0.31	2.9
rehydrated [b]	14	86	–	–	250	0.28	2.3
calcined [b]	–	–	–	–	270	0.38	3.0
CG	3	13	42	42	0.1	–	–
FCAL	6	34	32	28	52	0.05	2.4
rehydrated [a]	3	33	37	27	88	0.08	2.5
calcined [a]	–	–	–	–	98	0.11	2.3
rehydrated [b]	4	34	37	25	93	0.08	2.2
calcined [b]	–	–	–	–	95	0.10	2.3

[a] Rehydration condition: pH 9.0.

[b] Rehydration condition: pH 1.5.

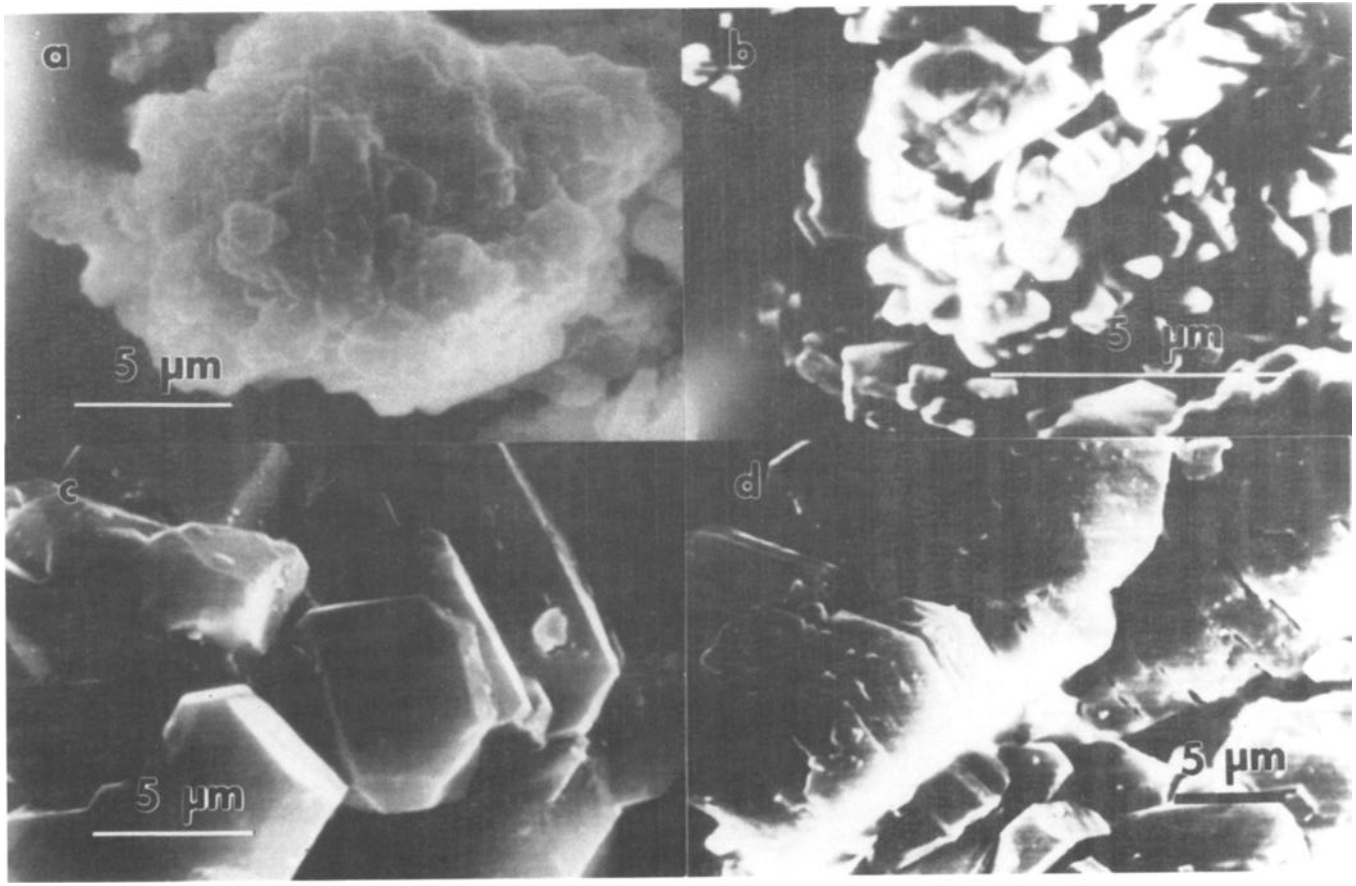

Fig. 2. Scanning electron micrographs of samples of (a) initial FG, (b) FG-FCAL, (c) initial CG and (d) CG-FCAL.

blocks, but only to the appearance of parallel cracks on their surface due to partial loss of interlayer water.

In concordance with the above XRD and SEM results are the DTG data presented in fig. 3. DTG curves of the initial samples of gibbsite (curves a and c) are similar. The first effect at 240°C is attributed to partial dehydration to Bö. The most intensive peak at 310°C is probably due to the slow dehydration of the main amount of gibbsite to χ-Al_2O_3, whereas the less pronounced peak at 540°C corresponds to the dehydration of Bö to γ-Al_2O_3 [10]. For the DTG curve of the FG-FCAL sample (curve b), however, only one low intensity peak appears at 285°C. In contrast, the gibbsite dehydration trend is retained for the CG-FCAL sample (curve d). TG curves for the FCAL samples show that for FG approximately 30% of the structural water is depleted from the structure, while for the CG sample it is only around 9%. Thus, in the case of the FG-FCAL sample, a metastable and X-ray amorphous product is obtained with a stoichiometry close to that of Al_2O_3, while for CG-FCAL a stoichiometry similar to the initial trihydrate is retained.

On the basis of the above analysis, we can outline the principal differences in the behavior of the "fine" and "coarse" particles in the heating zone and suggest a mechanism (fig. 4). For the FG particles, the residence time in the heating zone and the heating rate are sufficient to achieve uniform temperature over the entire particle volume. Thus, as illustrated in fig. 4a, the water vapor diffusion takes place between the layers of the gibbsite crystal. The rate of migration of the water molecules toward the particle surface (direction c) is smaller than the rate of water vapor pressure increase. Consequently, the internal vapor pressure reaches a criti-

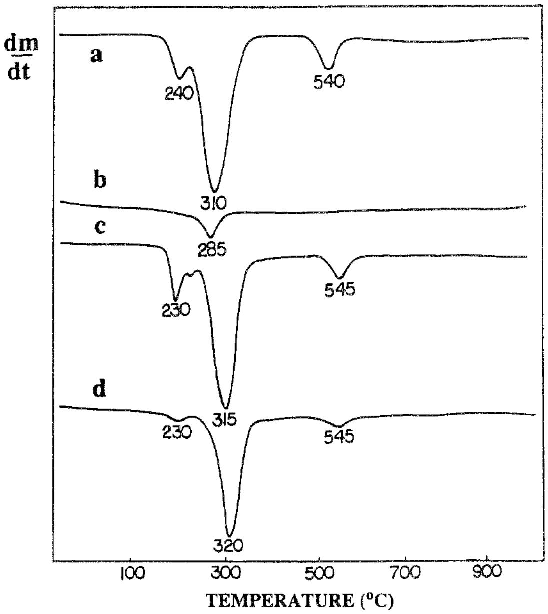

Fig. 3. DTG curves of samples of (a) initial FG, (b) FG-FCAL, (c) initial CG and (d) CG-FCAL.

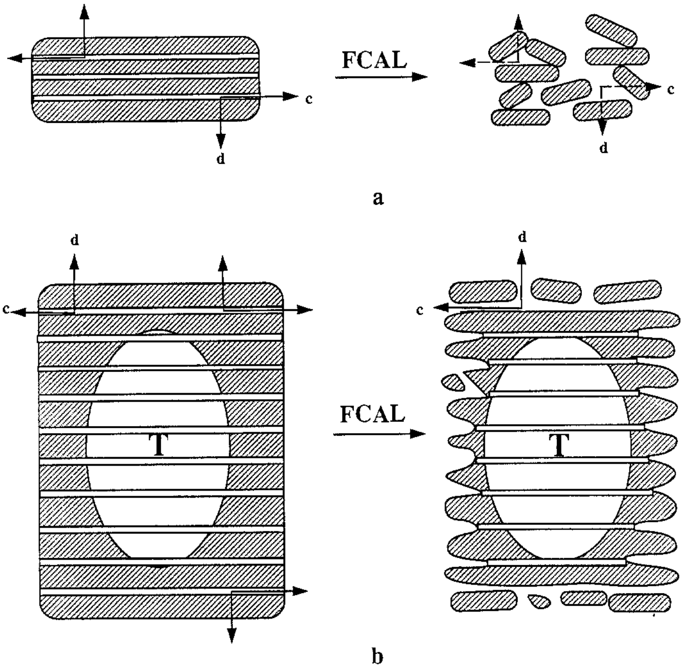

Fig. 4. Schematic representation of FCAL process of (a) FG particle, and (b) CG particle.

cal value, sufficient to fracture the particles in direction d, perpendicular to the layer plane, and a chaotic rearrangement of the product (fig. 2b) with an X-ray amorphous structure is observed.

In contrast, the CG particles experience a significant temperature gradient resulting in the establishment of an internal zone (fig. 4b). The temperature in this zone, denoted as *T*, is much lower than that of the surrounding area and the internal water vapor pressure cannot achieve a critical value. This leads to partial dehydration and particle fracture only at sites close to the external surface area. The large portion of the internal particle volume, however, is locked in the *T*-zone, where the initial gibbsite structure is retained. As a result, hydrothermal conditions are created at the border of the *T*-zone leading to the formation of some Bö-phase.

On the basis of the above we can anticipate important differences in the reactivity (rehydration ability) of the FG- and CG-FCAL samples. This can be illustrated by comparing X-ray diffractograms of the rehydrated products presented in fig. 5. Upon rehydration of the X-ray amorphous FG-FCAL sample at pH 9 and at pH 1.5, well-defined peaks appear that are characteristic for bayerite (Ba) and boehmite (Bö), respectively (curves a and b). These results are in agreement with the literature data [11]. However, the rehydration of the CG-FCAL sample (curves c and d) does not result in formation of Ba of Bö phases. The X-ray diffractograms are similar to those of the initial gibbsite, except for the appearance of small

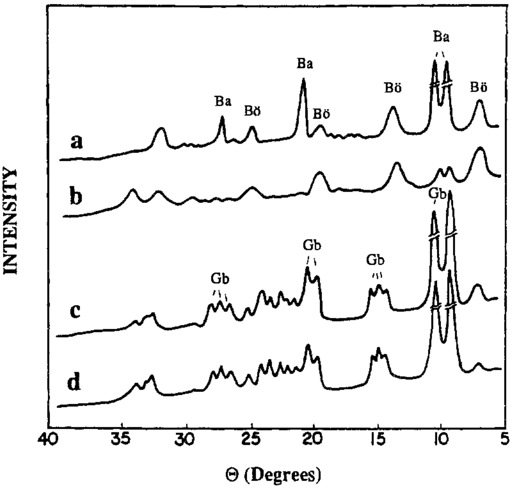

Fig. 5. X-ray diffractograms of FG-FCAL sample rehydrated at (a) pH 9.0, (b) pH 1.5 and CG-FCAL sample rehydrated at (c) pH 9.0 and (d) pH 1.5.

amount of the Bö at pH 9 (curve c). Thus, it is obvious that the rehydration of the FCAL samples strongly depends on the initial gibbsite grain size.

The DTG curves of the rehydrated samples in fig. 6 further illustrate the importance of grain size. Curve a for the rehydrated FG-FCAL sample at pH 9.0 shows

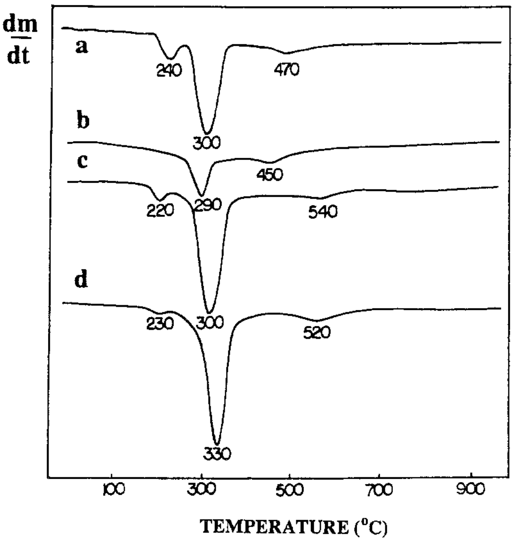

Fig. 6. DTG curves of FG-FCAL sample rehydrated at (a) pH 9.0, (b) pH 1.5 and CG-FCAL sample rehydrated at (c) pH 9.0 and (d) pH 1.5.

dehydration behavior typical of Ba, while curve b for rehydration at pH 1.5 is typical for Bö [15]. The TG curves of the above samples show 27% water loss for the sample rehydrated at pH 9.0, and around 17% for the sample rehydrated at pH 1.5. The water loss is somewhat lower than expected for pure Ba (35%), due to the simultaneous existence of some Bö phase. In contrast, the analogous rehydration conditions when applied to the CG-FCAL sample, afford DTG curves similar to those for the initial gibbsite (figs. 3c and 3d).

Nitrogen adsorption isotherms for the FCAL, rehydrated and outgassed at 550°C samples are given in fig. 7. Pore structure parameters are presented in table 1. Both initial gibbsite samples, FG and CG are characterized by very low specific surface area ($<2\,m^2/g$). The isotherms for the FG- and CG-FCAL samples (curves a and a′) exhibit weakly expressed type H4 hysteresis loops [13], due to the formation of some slit-shaped mesopores upon FCAL. In addition, the specific surface area increase up to two orders of magnitude, and the appearance of mesopores ($d_{p,max}$) confirm the formation of a mesoporous structure, which is not present for the initial samples. Remarkable differences appear in the course of the adsorption isotherms of FCAL and rehydrated samples. This is most pronounced for the FG sample as evidenced by the gradual transition of the type of hysteresis loops from H4 (curve a) to H3 (curve c) and to hybrid H1–H3 type (curve b). The above trend is accompanied by a significant increase of the particle size, a_{sBET} and V_p. This implies that the pore structure parameters of the rehydrated FG-FCAL gibbsite can be varied by controlling the pH. As expected for the CG-FCAL sample, the

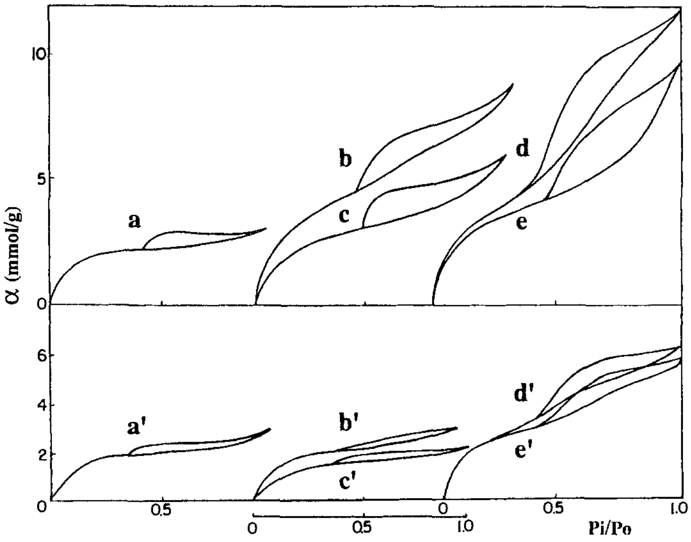

Fig. 7. Nitrogen adsorption isotherms of FG samples (a–e) and CG samples (a′–e′). Samples were treated as follows: (a and a′) FCAL; (b and b′) rehydrated at pH 1.5; (c and c′) rehydrated at pH 9.0; (d and d′) the same as (b and b′) plus calcination; (e and e′) the same as (c and c′) plus calcination.

course of the adsorption isotherms, the type of the hysteresis loops, the particle size, a_{sBET} and V_p is unaffected by rehydration pH (curves a′, b′, c′, and table 1).

The calcination of the rehydrated samples at 550°C results in the shift of the hysteresis loop toward higher α and p_i/p_0 values (curves d, e and d′, e′) and a corresponding increase of the a_{sBET}, V_p and $d_{p,max}$ due to the oxide formation. Again, essential differences in the pore structure appear depending on the initial grain size. For the FG-FCAL sample, rehydrated at both pH values, AAO is obtained as characterized by predominantly H1 type of hysteresis loops (cylindrical mesoporosity), high a_{sBET}, V_p and $d_{p,max}$. For the CG-FCAL sample, however, the hysteresis loops are much less pronounced and still of predominantly H3 type with little or no increase in the pore structure parameters. Therefore, the activation products of the CG cannot be called "active" or AAO.

In conclusion, the porous characteristics of the prepared alumina strongly depend on the initial grain size of the gibbsite and to a lower extent on the rehydration conditions chosen. Also, it should be mentioned that AAO obtained by FCAL of fine grain size gibbsite (< 50 μm), possess pore structure parameters similar to those of the commercial precipitated alumina adsorbents and catalysts. This leads us to believe that AAO, prepared from fine grain size gibbsite by flash calcination and purposeful rehydration can be used successfully as an adsorbent and catalyst support for petroleum industry.

Acknowledgement

The authors are grateful to Professor T.J. Pinnavaia for valuable discussions and comments.

References

[1] A.R. Birkin, ed., *Critical Reports on Applied Chemistry*, Vol. 20 (Wiley, New York, 1987) p. 3.

[2] V.A. Dzisko and A.S. Ivanova, Izv. Sib. Otd. Akad. Nauk SSSR, Ser. Khim. 5 (1985) 110 (in Russian).

[3] M. Inoue, K. Kitamura, H. Tanino, H. Nakayama and T. Inui, Clays Clay Miner. 37 (1989) 71.

[4] N.V. Maltzeva and G.M. Belotzercovskii, Zh. Prikl. Khim. 56 (1983) 1009 (in Russian).

[5] B.P. Zolotovskii, S.M. Paramzin, V.I. Zaikovskii, R.A. Buianov, L.M. Pliasova, V.E. Loyko and G.S. Litvak, Kinet. Katal. 31 (1990) 662.

[6] D. Papee and R. Tertian, Bull. Soc. Chim. France 5 (1955) 983.

[7] J. Rouquerol, F. Rouquerol and M. Gauteaume, J. Catal. 36 (1975) 99; 57 (1979) 222.

[8] Yu.K. Vorob'ev, B.N. Badaev, G.I. Lubishko, E.A. Levitskii, G.K. Boreskov, M.M. Andrushkevich, B.A. Baum, N.A. Pakhomov and L.G. Khomyakova, US Patent 4,166,100 (1979).

[9] U.K. Vorobev, R.A. Shkrabina, E.M. Moroz, V.B. Fenelonov, R.V. Zagrafskaia, T.D. Kambarova and E.A. Levitzkii, Kinet. Katal. 22 (1981) 1275.

[10] U. Bollmann, K. Becker, H.-J. Berger, P. Birke, S. Engels, G. Gruhn, K. Hancke, P. Kraak,

R. Lange and U. Steinike, Cryst. Res. Technol. 23 (1988) 1303.
[11] R.A. Shkrabina, E.M. Moroz, T.D. Kambarova, L.G. Homiakova, T.G. Bichkova and E.A. Levitzkii, Kinet. Katal. 22 (1981) 1281.
[12] G.M. Bliznakov, I.V. Bakardjiev and E.M. Gocheva, J. Catal. 18 (1970) 260.
[13] K.S.W. Sing, D.H. Everett, R.A.W. Haul, L. Moscou, R.A. Pierotti, J. Rouquerol and T. Siemieniewska, Pure Appl. Chem. 57 (1985) 603.
[14] W.B. Innes, Anal. Chem. 29 (1957) 1069.
[15] J.H. De Boer, J.M.H. Fortuin and J.J. Steggerda, Proc. Kon. Ned. Akad. Wet. Ser. B 57 (1953) 170.